The Effect of Optical Prepulse on Direct-Drive Inertial Confinement Fusion Target Performance

Introduction

In direct-drive inertial confinement fusion (ICF), laser light directly irradiates a capsule with a pulse of less than 10-ns duration. Laser ablation of material from the capsule surface produces extreme pressure that drives the implosion of the thermonuclear fuel. Ignition target designs[1–3] require a temporal pulse shape tailored to produce two or more converging shocks that coalesce in the imploding core. Ideally, the implosion occurs without premature heating of the shell or the fuel contained within because preheat reduces the implosion efficiency. Since ICF targets are inherently Rayleigh–Taylor (RT) unstable, it is particularly important to direct-drive ICF that the target perturbations produced by irradiation nonuniformities[3] are minimized. Another method to ameliorate the effects of this instability is to enhance ablative stabilization[3] by judiciously preheating the shell with shocks produced by the rise of the drive pulse. Successful ICF implosions therefore require precise control of the temporal shape of the drive intensity and minimal perturbations of the shell by that drive.

Typically drive pulses start with a low-intensity (~2%) "foot," several nanoseconds before the peak drive occurs. This foot is essential for producing the correct isentrope of the imploding target, i.e., one with sufficient heating to help stabilize the target but not high enough to greatly reduce its hydrodynamic efficiency. The simulations typically assume perfect optical contrast (i.e., no prepulses before the drive pulse begins). ICF lasers have high gain and experience significant saturation around the peak of the pulse; thus, low-level noise in the driver can readily produce prepulses. Since hydrodynamic target simulations generally cannot correctly model the effects of prepulses at less than 10^{-5} of the peak power, the specifications for optical contrast must be determined experimentally using target performance.

Implosion experiments[4,5] and theoretical calculations[6] carried out using 1054-nm lasers generally found that prepulse levels had to be kept eight to nine orders of magnitude below the peak power to obtain maximum performance (neutron yield). Corresponding optical measurement techniques[7,8] were also developed at that time. Since then ICF lasers and targets have changed significantly, but no new reliable experimental data exists on the effect of prepulses on target performance. Today, direct-drive targets are usually coated with a thin ($\leq$1000-Å) Al layer that retains the hydrogen isotopes in the gaseous fuel and prevents target damage caused by filamentation of laser light inside the target shell prior to plasma formation.[9,10] This layer can be compromised easily by low-energy optical prepulses. Most modern ICF lasers are frequency-tripled (351-nm) Nd:glass lasers that benefit greatly from the prepulse suppression afforded by the frequency conversion. Recently Elton *et al.*[11] suggested that prepulses on the OMEGA laser system[12] might be higher than expected, prompting the implementation of a contrast-monitoring system on OMEGA. This work presents the measured prepulse levels on OMEGA and a contrast criterion for OMEGA direct-drive implosions. Similar contrast criteria will apply to direct-drive experiments on the National Ignition Facility (NIF).[13]

In this article several techniques for characterizing prepulses on OMEGA and their effect on target performance (i.e., neutron yield) are presented. The results indicate that the upper limit for the allowable prepulse on target is ~0.1 J/cm^2 at peak intensities of $\leq 10^8$ W/cm^2. This translates to an intensity contrast of ~10^7 between the allowable prepulse and the peak of the main laser pulse. This limit is most relevant for Al-coated targets. The allowable prepulse may be higher for uncoated targets if such targets should prove viable in the future.

Optical Diagnostics and Their Interpretation

Optical contrast on OMEGA is measured at two places: (1) a UV contrast station located after the frequency converters and just ahead of the target chamber, and (2) an IR contrast station at the input to the amplifier chain, ahead of the first beam splitter on OMEGA. In both cases, the full beam aperture is sampled. The contrast is measured using fast vacuum photodiodes (Hamamatsu, R1328U-01-S-1 and R1328U-02-S-20) and high-speed oscilloscopes (TEK7250 or IN7101). A schematic layout of the UV contrast station is shown in Fig. 81.31. An air breakdown region is included in the design to protect the

diodes against damaging fluences during the main pulse. The prepulse monitors are calibrated with removable filters. These filters allow the main laser pulse to be fully measured on calibration shots that are typically performed daily. Removing these filters accesses the low-intensity prepulse region within 20 ns before the main laser pulse. The calibration filters have an optical density (OD) of 5.3 in the UV (2.9 in the IR), and, when removed, the detection threshold is typically around 8 orders of magnitude below the peak UV power (~5 to 6 orders of magnitude below the IR peak power). Extensive precautions have been taken to block stray light from affecting the measurements, including the spatial-filter aperture shown in Fig. 81.31. The temporal resolution of this system is better than 200 ps.

Typical prepulse records for a full-power OMEGA laser pulse are shown as the lower two curves in Fig. 81.32. The respective calibration curves with filters inserted are shown in the upper portion of this figure. (Note that their peaks are normalized to 1.) An IR prepulse (or prepulses) can be seen rising to ~10^{-4} of the peak IR power within ~1 ns of the arrival of the main pulse (the steep rise at $t = 0$). The corresponding UV power is <10^{-7} of the peak UV power. The difference in contrast level between the IR and UV pulses results from both the unsaturated gain in the IR system and the nonlinear frequency conversion. [Low-power prepulses experience small-signal conversion $\left(I_{UV} \propto I_{IR}^{3}\right)$, whereas the conversion is almost linear with the intensity near the peak of the pulse.] From simulations and experiments we have found that the prepulse contrast ratio obeys a heuristic relationship of $C_{UV} \propto (C_{IR})^2$, where $C = P_{peak}/P_{prepulse}$ (the subscripts refer to the peak and prepulse powers). This relationship is born out in the results shown in Fig. 81.32, where the UV prepulse level is mostly below the noise limit, i.e., flat portions of the trace. (The flat lines for $t > 0$ are the saturated diode signals.) The UV prepulse ($P_{prepulse} < 10^{-7}\ P_{peak}$) within the last nanosecond before the onset of the main pulse is very close to the detection threshold.

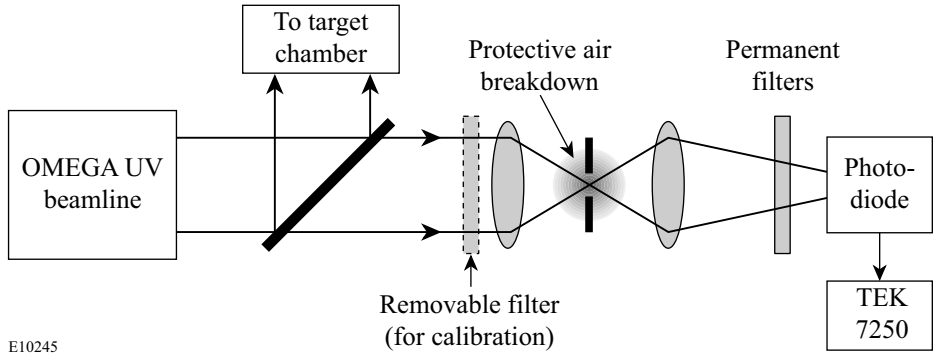

Figure 81.31
Schematic layout of the UV contrast monitor station. To protect the photodiode the confocal lens pair breaks down the air when the high-intensity laser pulse arrives. The removable filter pack is inserted for calibration of the prepulse monitor.

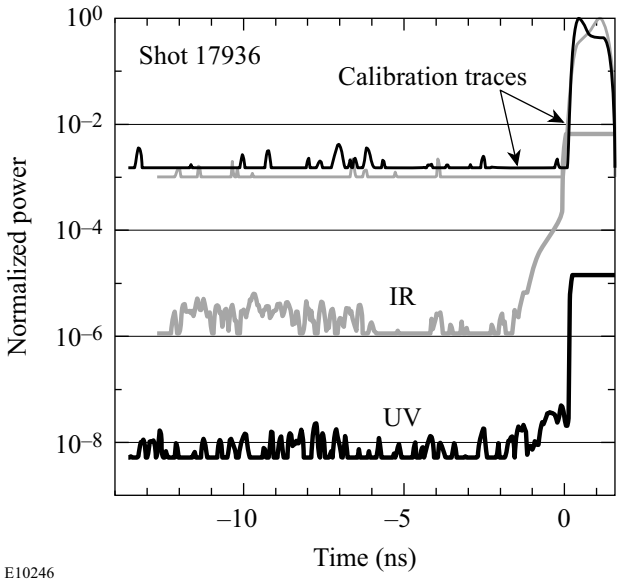

Figure 81.32
Contrast monitor traces for the UV at the output and the IR at the input to OMEGA. The thin traces on top show the calibration traces with the main pulses on scale and normalized. The thick lower traces are taken without the calibration filter (see Fig. 81.31) and permit prepulse monitoring to a contrast of 10^{-8} from the peak in the UV (10^{-6} from the peak in the IR). No prepulses are seen above the noise for times $t < -2$ ns.

The prepulse within 1 ns of the main pulse originates in either the regenerative amplifier (regen) or the pulse-shaping system before the regen. Such prepulses are only marginally affected by the Pockels cells following the regen. The general shape and position of these prepulses are reproducible although the intensity fluctuates, particularly in the UV. These observations rule out regen amplified stimulated emission (ASE), leaving spurious intracavity reflections within the regen or imperfections in the laser pulse injected into the regen as likely sources. The exact prepulse source is still under investigation.

A large number of OMEGA shots have been examined for UV prepulses; it was found that none had a prepulse in excess of 10^{-8} of the peak pulse within the time window of −17 ns and −1 ns prior to the main pulse. Within the last nanosecond the contrast degrades but the prepulse level typically does not exceed 10^{-6} of the main pulse (the corresponding cumulative time-integral of the intensity or the fluence is about 0.2 J/cm^2 in the prepulse) and in most cases remains at or below 10^{-7}.

Apart from UV prepulses, additional prepulses on target could be due to IR and green laser light left over from the frequency-conversion process. In each of OMEGA's 60 beams, the frequency converters are followed by two dielectric multilayer mirrors, each with nearly 100% reflectivity at 351 nm and average reflectivities of ~6% in the IR and ~10% in the green. The residual green energy is always much smaller (1%–5%) than either the UV or IR energies and can therefore be neglected. The IR intensity on target is reduced by a factor of ~280 because of the IR transmission of the UV mirrors. The chromatic shift of the OMEGA lenses produces IR spots of ~15-mm diameter in the target plane. Since the random phase plates[14] produce a UV focal spot with a FWHM of 0.5 mm and do not measurably affect the IR spot size, the IR on-target intensity is reduced by an additional factor of 900 because of this chromatic defocusing. Since there is no IR prepulse monitor at the laser output, we must estimate the IR output prepulse from the measured UV prepulse. Assuming small-signal, third-harmonic conversion efficiency for the IR prepulse [$P_{IR,out} \approx (P_{UV,out})^{1/3}$], we find that the IR on-target prepulse contrast is approximately $C_{IR,on\text{-}target} = \sim 900 \times 280 \times (C_{UV})^{1/3}$, which is $\sim 8 \times 10^7$, when the UV contrast is $\sim 3 \times 10^7$ as obtained from Fig. 81.32. Making the pessimistic assumption of 50% third-harmonic conversion efficiency for the main pulse, we find that the IR energy prepulse on target is ~1/3 of the UV prepulse energy.

An independent estimate of the IR on-target prepulse level (or contrast) can be obtained from the IR input prepulse monitor, the ten-fold deterioration of the IR contrast due to the gain saturation in the amplifiers, and the small-signal UV conversion efficiency. Since the IR output energy can be as high as the UV energy (depending on pulse shape and duration), one can obtain an upper limit for the IR prepulse intensity on target as $I_{IR,on\text{-}target,prepulse} < [10/(900 \times 280 \times C_{IR,input})] \times I_{UV,peak\ on\text{-}target} \approx (4 \times 10^{-5}/C_{IR}) \times I_{UV,peak\ on\text{-}target}$. For $C_{IR,input} \approx 1.5 \times 10^4$ (Fig. 81.32) the upper estimate for the IR prepulse is $I_{IR,on\text{-}target,prepulse} < 10^{-8}\ I_{UV,peak\ on\text{-}target}$, which is still well below the corresponding measured UV prepulse level $\approx 5 \times 10^{-8}$ in Fig. 81.32. The two estimates of the on-target IR prepulse level (shot 17936, Fig. 81.32) lie within a factor of ~4, consistent with the accuracy of these estimates.

Threshold Experiments

The thin Al coatings (0.1 μm) applied to all imploding targets on OMEGA are particularly susceptible to damage due to prepulses. To determine if prepulses had any effect on these layers, their integrity (reflectivity) was optically probed from $t \simeq 15$ ns up to the arrival of the main pulse ($t = 0$). The experimental configuration for those measurements is shown schematically in Fig. 81.33. An Al-coated flat CH target was irradiated with one or six beams symmetrically arranged around the target and at ~20° with respect to the target normal (see Fig. 81.33). The Al coating was also used as one mirror of an interferometer whose fringes were temporally resolved with a streak camera.* The interferometer was illuminated with a 10-ns, second-harmonic pulse (532 nm) of a Nd:YAG laser.

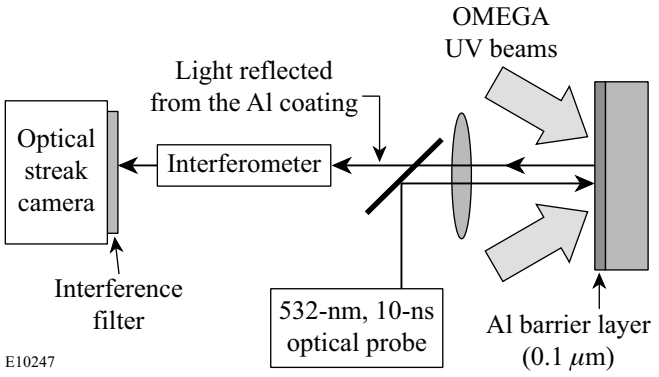

Figure 81.33
Schematic experimental setup for measuring the integrity of thin Al surface layers prior to irradiation with one or six OMEGA laser beams. The Al layer on the target acts as one end mirror for the interferometer. The target and the fringes are imaged onto a streak camera to monitor the integrity (reflectivity) of the Al. An interference filter, which protects the streak camera against excessive stray light, is required for high fringe contrast.

*This instrument [the active shock breakout (ASBO) instrument] was developed and installed on OMEGA by the Lawrence Livermore National Laboratory.

Figure 81.34 shows streaked interferometer images for two shots with Al-coated (0.1 μm) plastic targets (20 μm) irradiated with 1-ns square-top UV pulses containing 90 J (top image) and 2.7 kJ (lower image). The OMEGA beams were outfitted with phase plates[14] that produce a spot size (FWHM) of 0.5 mm. Smoothing by spectral dispersion (SSD) was not used; OMEGA was operated with narrow bandwidth. The probe beam for the interferometer was timed primarily to determine if early prepulses ($t \leq -10$ ns) were present, as suggested by Elton *et al.*[11] The beam energies for shot 16882 produced an intensity of 8×10^{14} W/cm^2 on target, which is similar to that used for spherical implosion shots. (These intensities are averaged over the envelope of the beam; the actual peak intensities in the speckles can be 4 to 5 times higher.[15]) Shot 16881 (Fig. 81.34, top image) was a low-energy shot to test the instrument under conditions where any prepulses (if present) were expected to be below the damage threshold for the Al coating; no change in reflectivity was observed. (Note that the streak camera trigger was adjusted between the two shots in Fig. 81.34, explaining the lack of early data for shot 16881. Furthermore, the interferometer illumination beam came ~1 ns earlier in shot 16882 compared to shot 16881.)

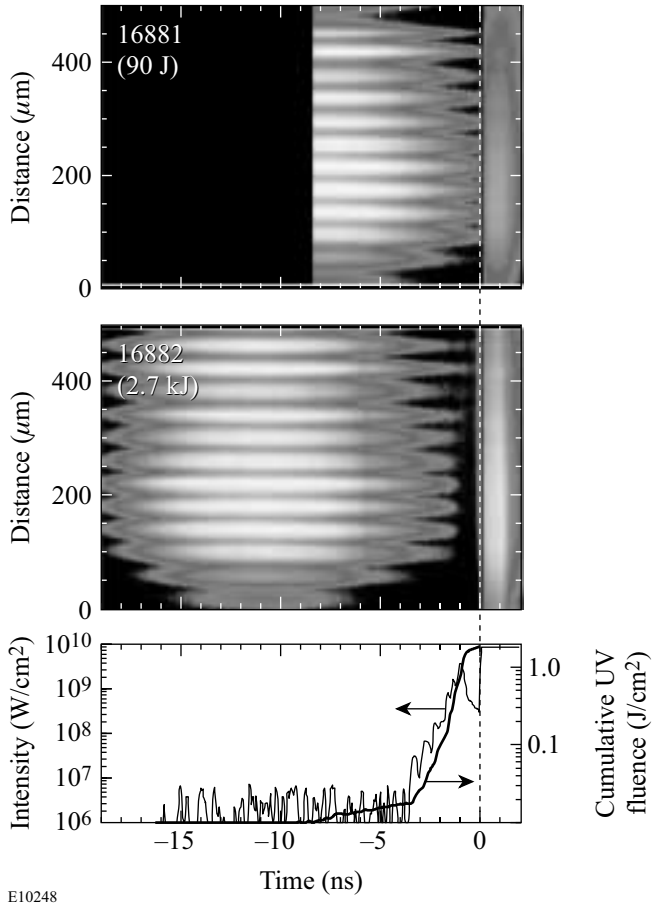

Figure 81.34
Streaked interferometer fringes for two different irradiation conditions. Upper image: A low-energy shot shows interference fringes leading right up to the start of the main laser pulse. The signal to the right of $t = 0$ is due to plasma self-emission. Lower image: A high-energy shot under OMEGA implosion conditions ($I \sim 10^{15}$ W/cm^2). The two traces are the measured UV prepulse intensity on target and the cumulative fluence on target for shot 16882. The absence of fringes in the lower part of the lower image indicates complete disruption of the Al layer at fluences ≥ 1 J/cm^2.

As seen in Fig. 81.34, the streaked interferometer image of shot 16882 shows no evidence of an early (-16 ns $< t < -2$ ns) prepulse affecting the Al surface. There is also no evidence of a prepulse in the corresponding UV diode trace for that shot. The latter, which was normalized to the peak UV intensity on target, is plotted in the graph directly below the image. The cumulative time integral (i.e., fluence) is shown in the bottom trace. This level of prepulse is higher than typical OMEGA performance but is useful because it allowed the measurement of the effects a prepulse has on the Al layer. The interferometer fringes completely disappear once the cumulative prepulse fluence reaches ~1 J/cm^2 ($t \approx -1$ ns in Fig. 81.34), corresponding to a prepulse intensity of $\sim 2 \times 10^9$ W/cm^2. Figure 81.34 also shows that the fringe contrast degrades well before the fringes disappear completely. It is likely that the disruption of the Al surface is not spatially uniform, and one expects a gradual decrease in fringe visibility as the Al layer is destroyed. Unfortunately the images in Fig. 81.34 do not allow a precise evaluation of the prepulse fluence or the intensity at which the disruption of the Al layer begins. These measurements are therefore supplemented with others to determine the effect prepulses have on target damage and target performance (see below).

Aluminum-Barrier-Layer Damage Threshold

Measurements of the UV breakdown threshold[16] of thin barrier layers coated on plastic targets were carried out on LLE's tabletop terawatt laser system.[17] To provide relevant interaction conditions, the output from the 1-μm-wavelength, Nd:glass laser system was frequency tripled to 351 nm and focused onto the targets with a 60-cm-focal-length lens (f number ~9) after passing through a binary distributed phase plate.[14] In these experiments, the first minimum in the Airy pattern had a 380-μm diameter, and the characteristic speckle size was ~3 μm. The experiments were carried out with 1.4-ps and 40-ps Gaussian laser pulses.

The target disruption (surface breakdown) was measured by a change in transmission through the target as a function of laser fluence. An example of the results is shown in Fig. 81.35, where the transmission as a function of laser fluence is shown for a 15-μm-thick parylene target coated with 0.02 μm of Al. The transmission was normalized to the transmission of the optical system in the absence of a target. The data show that the transmission begins to decrease when the fluence exceeds ~0.1 J/cm^2 (defined as the damage fluence). The transmission data for both the 1.4- and 40-ps pulses were found to be indistinguishable, confirming that laser fluence, rather than intensity (factor of ~30 difference), determines the breakdown threshold. Other metal coatings show similar behavior.

Microscopic inspection of targets exposed to single shots showed damage to the plastic (CH) substrate at twice the threshold for observable changes in transmission.

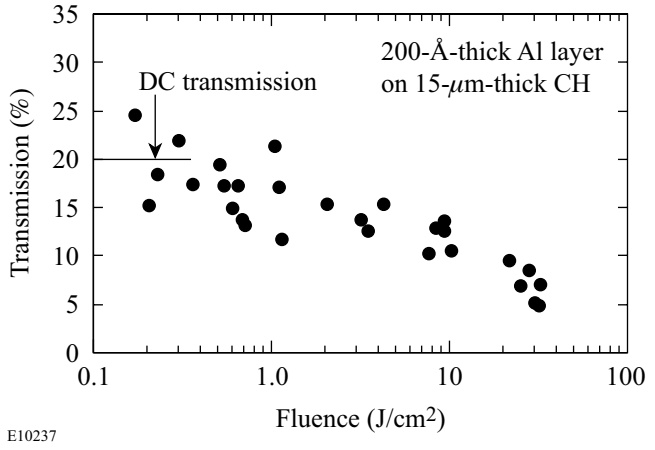

Figure 81.35
The UV transmission as a function of laser fluence for a 15-μm-thick parylene target coated with 0.02 μm of Al. The transmission begins to decay at fluence levels above 0.1 J/cm^2.

Target Performance

The effect of prepulses on capsule implosions was investigated with a series of 17 OMEGA implosions. The imploding capsules were of nearly identical diameter (896 to 908 μm) and wall thickness (19.6 to 20.5 μm) and were filled with 10 atm of D_2. Their shells consisted of an outside CH layer ranging in thickness from 14 to 19.6 μm with an inner CH layer doped with 1% Si with a thickness ranging from 0 to 8.8 μm. All capsules were coated with 0.1 μm of Al. Two pulse shapes of 3-ns overall duration were used in these shots; one had a foot of 1 ns at the half peak intensity while the other had a similar foot at 1/8 of the peak. SSD beam smoothing was used on all shots. The on-target UV energy ranged from 17 to 19.5 kJ for these experiments.

The prepulse monitor was used to characterize the prepulse power on these shots. The fluence was determined from the cumulative integral of that power. A scintillator-photomultiplier detector at a distance of 3 m from target center measured the DD neutron yield on these shots.

To characterize the neutron yield performance for these experiments the yields for each pulse shape and target combination were normalized to the highest neutron yield shot with that combination. In Fig. 81.36 these normalized neutron yields are plotted as a function of the measured prepulse fluence. In general, target shots with lower prepulse levels outperform those with higher prepulse levels. From this limited set of data it appears that prepulse fluence levels in excess of 0.2 J/cm^2 cause a reduction of the neutron yield by a factor of 2 compared to shots with lower prepulse levels.

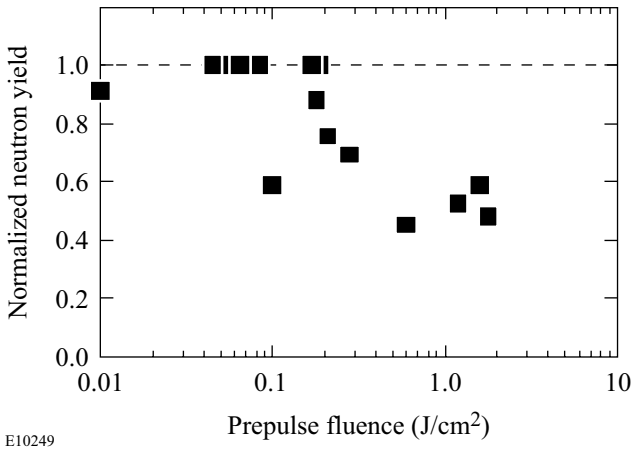

Figure 81.36
Normalized neutron yield as a function of prepulse fluence level (J/cm^2) indicates degraded target performance for prepulse fluences above 0.2 J/cm^2.

Discussion

This work quantifies the on-target irradiation contrast of the OMEGA laser and establishes an acceptable prepulse fluence criterion for high-performance ICF implosions. Of primary concern was the assertion[11] that, 5 to 10 ns prior to the main laser pulse, OMEGA produces prepulses that lead to plasmas with electron temperatures exceeding 100 eV. A prepulse monitor subsequently installed on OMEGA indicates that no prepulses have been observed between 20 ns and ~2 ns before the arrival of the main pulse; however, in the final 1 to 2 ns

before the main laser pulse, OMEGA occasionally produces a prepulse that can affect target performance.

The photodiodes that monitor the prepulse contrast in both the initial IR and final UV portions of the system are cross calibrated to the main laser pulse. The corresponding prepulse sensitivities are 10^{-6} and 10^{-8} below the main pulse intensity. Experiments that optically probe the integrity of thin Al coatings using interferometry demonstrate that the 0.1-μm Al layers are completely destroyed by prepulse fluences in excess of 1 J/cm^2. Independent transmission measurements on plastic targets with 0.02-μm Al layers (Fig. 81.35) indicate that the transmission through these Al layers is altered when the incident fluence exceeds 0.1 to 0.2 J/cm^2. Damage to the plastic substrate was typically observed, however, at two times higher fluences.

The neutron yields of imploding targets (Fig. 81.36) indicate that prepulse fluences of $\geq$0.2 J/cm^2 measurably affect and decrease target performance. This prepulse "threshold" fluence is consistent with that necessary to change the transmission through thin Al layers (Fig. 81.35). This threshold fluence is significantly lower than that required to completely destroy the fringe contrast of the interferometer experiments testing the integrity of the Al layer (Fig. 81.34). The interferometer experiments show decreased contrast, however, well before the fringe visibility disappears completely. Thus the transmission experiments and the interferometer experiments support each other and are consistent with the target performance data. We conjecture that the small-scale perturbations in the Al surface layer likely serve as seed for the RT instability during the ablation phase of the implosion. These perturbations are thus amplified to levels that affect the symmetry of the implosion and thus reduce the neutron yield.

Conclusions

The contrast monitors for the OMEGA laser system are capable of sensing UV prepulses that are $\geq 10^{-8}$ of the main laser pulse. Our observations indicate that the prepulse level is below the detection threshold of 10^{-8} of the main pulse for all shots up to ~2 ns before the onset of the main pulse. During the last 1 or 2 ns before the main pulse, OMEGA intermittently produces prepulses up to 10^{-6} of the main-pulse intensity (with a fluence ~0.2 J/cm^2). The source of this problem is under investigation.

Optical probe experiments using interferometry show that the thin Al layers on the target surface maintain measurable fringe visibility until the prepulse fluence reaches ~1 J/cm^2, which is attained when the prepulse reaches $\sim 2 \times 10^{-6}$ of the peak laser power. These findings are consistent with independent transmission measurements on thin (0.02-μm) Al layers that exhibit decreased transmission at fluences exceeding 0.1 or 0.2 J/cm^2. Imploding targets also have decreased neutron yields for prepulse fluences exceeding 0.1 or 0.2 J/cm^2. This is believed to be the result of small-scale perturbations created by laser damage in the target surface.

From the experiments reported here we conclude that precision ICF experiments on OMEGA require that the cumulative prepulse fluences be kept below 0.2 J/cm^2 corresponding to an optical intensity contrast $\geq 10^7$ on OMEGA. Prepulse requirements for NIF direct-drive targets are expected to be similar to these requirements if Al barrier layers are necessary.

ACKNOWLEDGMENT

This work was supported by the U.S. Department of Energy Office of Inertial Confinement Fusion under Cooperative Agreement No. DE-FC03-92SF19460, the University of Rochester, and the New York State Energy Research and Development Authority. The support of DOE does not constitute an endorsement by DOE of the views expressed in this article.

REFERENCES

1. R. L. McCrory, R. E. Bahr, T. R. Boehly, T. J. B. Collins, R. S. Craxton, J. A. Delettrez, W. R. Donaldson, R. Epstein, V. N. Goncharov, R. Q. Gram, D. R. Harding, P. A. Jaanimagi, R. L. Keck, J. P. Knauer, S. J. Loucks, F. J. Marshall, P. W. McKenty, D. D. Meyerhofer, S. F. B. Morse, O. V. Gotchev, P. B. Radha, S. P. Regan, W. Seka, S. Skupsky, V. A. Smalyuk, J. M. Soures, C. Stoeckl, R. P. J. Town, M. D. Wittman, B. Yaakobi, J. D. Zuegel, R. D. Petrasso, D. G. Hicks, and C. K. Li, "OMEGA Experiments and Preparation for Direct-Drive Ignition on the National Ignition Facility," to be published in *Inertial Fusion Sciences and Applications 1999*, Bordeaux, France, 12–17 September 1999.

2. S. V. Weber *et al.*, *ICF Quarterly Report* **7**, 43, Lawrence Livermore National Laboratory, Livermore, CA, UCRL-LR-105821-97-2 (1997).

3. S. E. Bodner, D. G. Colombant, J. H. Gardner, R. H. Lehmberg, S. P. Obenschain, L. Phillips, A. J. Schmitt, J. D. Sethian, R. L. McCrory, W. Seka, C. P. Verdon, J. P. Knauer, B. B. Afeyan, and H. T. Powell, Phys. Plasmas **5**, 1901 (1998).

4. E. B. Goldman *et al.*, J. Appl. Phys. **45**, 1158 (1974).

5. J. M. Soures, T. C. Bristow, H. Deckman, J. Delettrez, A. Entenberg, W. Friedman, J. Forsyth, Y. Gazit, G. Halpern, F. Kalk, S. Letzring, R. McCrory, D. Peiffer, J. Rizzo, W. Seka, S. Skupsky, E. Thorsos, B. Yaakobi, and T. Yamanaka, in *Laser Interaction and Related Plasma Phenomena*, edited by H. J. Schwarz (Plenum Press, New York, 1981), Vol. 5, pp. 463–481.

6. Yu. V. Afanas'ev and O. N. Krokhin, Sov. Phys.-JETP **25**, 639 (1967).

7. J. Bunkenburg, J. Boles, D. C. Brown, J. Eastman, J. Hoose, R. Hopkins, L. Iwan, S. D. Jacobs, J. H. Kelly, S. Kumpan, S. Letzring,

D. Lonobile, L. D. Lund, G. Mourou, S. Refermat, W. Seka, J. M. Soures, and K. Walsh, IEEE J. Quantum Electron. **QE-17**, 1620 (1981).

8. G. Mourou, J. Bunkenburg, and W. Seka, Opt. Commun. **34**, 252 (1980).

9. J. E. Balmer, T. P. Donaldson, W. Seka, and J. A. Zimmermann, Opt. Commun. **24**, 109 (1978).

10. D. K. Bradley, T. Boehly, D. L. Brown, J. Delettrez, W. Seka, and D. Smith, in *Laser Interaction and Related Plasma Phenomena*, edited by H. Hora and G. Miley (Plenum Press, New York, 1991), Vol. 9, pp. 323–334.

11. R. C. Elton, H. R. Griem, and E. J. Iglesias, Bull. Am. Phys. Soc. **44**, 38 (1999).

12. T. R. Boehly, R. S. Craxton, T. H. Hinterman, P. A. Jaanimagi, R. L. Keck, J. H. Kelly, T. J. Kessler, R. L. Kremens, S. A. Kumpan, S. A. Letzring, R. L. McCrory, S. F. B. Morse, W. Seka, S. Skupsky, J. M. Soures, and C. P. Verdon, in *Proceedings of the IAEA Technical Committee Meeting on Drivers for Inertial Confinement Fusion*, edited by J. Coutant (IAEA, Vienna, 1995), pp. 79–86.

13. J. R. Murray, in *Third Annual International Conference on Solid State Lasers for Application to Inertial Confinement Fusion*, Supplement to *Proceedings of SPIE, Volume 3492* (SPIE, Bellingham, WA, 1998), pp. 1–10.

14. T. J. Kessler, Y. Lin, J. J. Armstrong, and B. Velazquez, in *Laser Coherence Control: Technology and Applications*, edited by H. T. Powell and T. J. Kessler (SPIE, Bellingham, WA, 1993), Vol. 1870, pp. 95–104.

15. H. A. Rose and D. F. DuBois, Phys. Fluids B **5**, 590 (1993).

16. Y. Fisher, T. R. Boehly, D. K. Bradley, D. R. Harding, D. D. Meyerhofer, and M. D. Wittman, Bull. Am. Phys. Soc. **43**, 1784 (1998).

17. Y.-H. Chuang, D. D. Meyerhofer, S. Augst, H. Chen, J. Peatross, and S. Uchida, J. Opt. Soc. Am. B **8**, 1226 (1991).